$$A_1 = [r_1 + \tau(r_3 - r)]A_4 - \tau(g_3 + g) \qquad (12c)$$

$$A_2 = \frac{\tau}{\sigma}\left[-\left(r_1 + \frac{\delta}{\tau}r_2 + \tau r_3 - \tau r\right)A_4 + (g_2 + \tau g_3 + \tau g)\right] \qquad (12d)$$

$$A_3 = [r_3 - (\tau/\sigma)r]A_4 - (\tau/\sigma)g \qquad (12e)$$

$$B_1 = (r - r_3)A_4 + (g_3 + g) \qquad (12f)$$

$$B_2 = [(r_1 + r_2 + \tau r_3 - \tau r)A_4 - (g_2 + \tau g_3 + \tau g)]/\sigma \qquad (12g)$$

$$B_3 = (rA_4 + g)/\sigma \qquad (12h)$$

$$C_1 = hGB_1 + r_1B_4 \qquad (12i)$$

$$C_2 = hGB_2 + r_2B_4 \qquad (12j)$$

$$C_3 = hGB_3 + r_3B_4 \qquad (12k)$$

where

$$g = \frac{m\sigma g_1 - \tau g_2 + (m^2\sigma^2 - \tau^2)g_3}{1 + \tau^2 - m^2\sigma^2}$$

$$r = -\frac{(m^2\sigma - \tau)r_1 - \delta r_2 + (m^2\sigma^2 - \tau^2)r_3}{1 + \tau^2 - m^2\sigma^2} \qquad (13)$$

The quantities g_1, g_2, and g_3 can be calculated in the following way, e.g.,

$$g_1 = -(1/k\rho_0 a_0 u_0)(\partial p_0/\partial\beta)(\partial\beta/\partial\theta)\dot{\theta}$$

where $\partial p_0/\partial\beta$ and $\partial\beta/\partial\theta$ can be obtained from Eq. (2), and $\dot{\theta}$ can be calculated if the wedge is assumed to oscillate harmonically according to

$$\theta = \theta_a(1 + \alpha \cos kt),\ |\alpha| < 1 \qquad (14)$$

It is seen from Eqs. (12–14) that the coefficients A_1 through B_4 and hence the first-order solution are proportional to the amplitude of oscillation. This is the same as in the case of small amplitude oscillations. What is different is, as pointed out in Ref. 2, that for large amplitudes the constants of proportionality depend on the instantaneous (quasi-steady) flow quantities, whereas for small amplitudes they depend on the mean flow quantities. Thus for large-amplitude oscillations the flowfield is highly nonlinear, as expected.

We shall now show that for the special case of hypersonic flow past a slender wedge the present solution reduces to that of Kuiken.[2] A comparison will be given of the pressure at the wedge surface derived by either theory. According to the present theory the pressure at the body surface is given by

$$\frac{\bar{p}_b}{\bar{p}_\infty\gamma M_\infty{}^2} = p_0 + k\rho_0 u_0[(A_1 + \delta B_1)x + C_1 - hHB_1] \qquad (15)$$

For hypersonic flow past a slender wedge, β and θ are all small, and when their quadratic terms are neglected, Eq. (15) can be simplified and put in a form directly comparable with Eq. (54) of Ref. 2. Thus

$$\bar{p}_b/\bar{p}_\infty = \gamma K^2(p_0/\beta^2)[1 + kA(Rx + Sh)] \qquad (16)$$

where

$$A = -\frac{\alpha \sin kt}{1 + \alpha \cos kt}\frac{K^2 - 1}{K^2 + 1} = -\frac{\alpha \sin(kt)(K_a{}^2 - 1)/2K_a}{\left[\left\{\frac{K_a{}^2 - 1}{2K_a}(1 + \alpha \cos kt)\right\}^2 + 1\right]^{1/2}} \qquad (17)$$

$$R = \frac{4\gamma(K^2 + 1)}{2\gamma K^2 - (\gamma - 1)}\left[1 + \frac{K^2}{K^2 + 1} \times \frac{(\gamma + 1)(K^4 - 1) - (3K^2 + 1)\{(\gamma - 1)K^2 + 2\}}{(\gamma + 1)(K^4 - 1) + (3K^2 + 1)\{(\gamma - 1)K^2 + 2\}}\right]$$

$$S = -4\gamma K^2/[2\gamma K^2 - (\gamma - 1)]$$

Now A and S are identical to the same quantities in Ref. 2, and R gives exactly the same values as those tabulated in Ref. 2. Hence Eq. (16) is identical to Eq. (54) of Ref. 2, and we may conclude that for the special case of hypersonic flow past a slender wedge, the present solution reduces to that of Kuiken. However, the present solution can be used for both hypersonic and supersonic flows past any wedges with attached bow shocks on both sides of the wedge.

References

[1] Hui, W. H., "Stability of Oscillating Wedges and Caret Wings in Hypersonic and Supersonic Flows," *AIAA Journal*, Vol. 7, No. 8, Aug. 1969, pp. 1524–1530.

[2] Kuiken, A. K., "Large-Amplitude Low-Frequency Oscillation of a Slender Wedge in Inviscid Hypersonic Flow," *AIAA Journal*, Vol. 7, No. 9, Sept. 1969, pp. 1767–1774.

Further Experimental Studies of Buckling of Electroformed Conical Shells

R. L. Sendelbeck*
Stanford University, Stanford, Calif.

AND

J. Singer†
Technion, Israel Institute of Technology, Haifa, Israel

In an earlier experimental investigation,[1] the validity of linear theory for buckling of conical shells under hydrostatic pressure was confirmed also for large taper ratios. Correlation of the critical pressures of conical shells with those of equivalent cylindrical shells[2–4] yields a curve (or curves) that have a "hump" at large taper ratios. Since Singer and Bendavid aimed at confirmation of the theory in the "hump" region, all the test specimens had fairly large taper ratios. The results for conical shells of large taper ratio were then correlated with previous tests on other conical shells and cylindrical shells (i.e., shells of zero taper ratio). It may be argued that for a higher degree of certainty, "control" specimens of small taper ratio from the same batch, or same manufacturing technique, should have been included. This motivated the present series of tests, which repeated tests similar to those of Ref. 1 but accompanied them with parallel tests of corresponding specimens of small taper ratio. The results reconfirmed and substantiated the findings of Singer and Bendavid.

The original test apparatus and procedure of Ref. 1 were employed after incorporation of some improvements. For better centering the original gallows (Fig. 3 of Ref. 1) was re-

Received April 6, 1970. This research was supported by the Air Force Office of Scientific Research, OAR, U. S. Air Force under Contract F44620-69-C-009.

* Director, Structures Laboratory, Department of Aeronautics and Astronautics.

† Professor, Department of Aeronautical Engineering. Associate Fellow AIAA.

Table 1 Correlation of test results with theory: cone angle $\alpha = 30°$ and $\nu = 0.3$; large end radius $R_2 = 5.00$ in. and $E = 24.9 \times 10^6$ psi

	Test no.	Specimen	Taper ratio ψ	h, in.	Small end radius R_1, in.	(R_1/h)	(ρ_{av}/h)	(l/ρ_{av})	Equivalent cylindrical shell, Eq. (3) $(\bar{p}/E) \times 10^8$
Short	1	S127	0.244	0.00350	3.78	1080	1450	0.481	2.476
Short	2	S130	0.244	0.00330	3.78	1145	1540	0.481	2.135
Short	3	S131	0.244	0.00377	3.78	1003	1340	0.481	2.985
Long	4	S126	0.750	0.00283	1.25	442	1280	2.08	0.768
Long	5	S129	0.750	0.00379	1.25	330	950	2.08	1.594
Long	6	S132	0.750	0.00374	1.25	334	960	2.08	1.542
Long	7	S133	0.750	0.00352	1.25	355	1030	2.08	1.326

			Test			Correlation with theory (Ref. 7) SS3 "classical" simple supports			SS4		
	Test no.	Specimen	$(p_{ex}/E) \times 10^8$	t	$g(\psi)$	$(p_3/E) \times 10^8$	t	$g(\psi)$	$(p_4/E) \times 10^8$	t	$g(\psi)$
Short	1	S127	2.758	19	1.11	2.510	20	1.01	3.338	24	1.36
Short	2	S130	2.370	19	1.11	2.160	21	1.01	2.910	24	1.36
Short	3	S131	3.520	18	1.18	3.019	20	1.01	4.042	23	1.35
Long	4	S126	1.127	11	1.47	0.934	12	1.22	1.314	15	1.71
Long	5	S129	2.460	9	1.54	1.937	11	1.22	2.712	14	1.70
Long	6	S132	2.405	8	1.56	1.874	11	1.22	2.623	14	1.70
Long	7	S133	2.024	11	1.53	1.611	11	1.22	2.256	14	1.70

placed by a standing type drill press (see Fig. 1). The bottom end fixture of the shell assembly was first placed on the base plate of the drill press. Its center then aligned with that of the drill press, and with a dial gage on a rotating arm the base plate was adjusted to be precisely perpendicular to the drill press axis. The specimen was then loosely fitted into the top fixture and the latter aligned with the bottom fixture by "chucking" into the drill press. As the loosely clamped shell was lowered onto the bottom fixture it seated itself in axial alignment with the whole assembly.

Since it was found that the tensioning of the end ring nuts affect the buckling load,[5] great care was taken to obtain uniform and equal tensioning in all the tests and all the shells were assembled by one person for better consistancy. All the shells in the present series were clamped down tighter than those in Ref. 1.

The specimens were made of nickel electroformed over the same aluminum mandrel as in Ref. 1. However, a different nickel plating solution, that had been developed since the earlier tests, was used. This bath had yielded nickel with consistent mechanical properties of $E = 24 \times 10^6$ psi and $\nu = 0.3$ for over 2 yr. The modulus of elasticity was checked by repeated tests of 3 coupons cut from the shells and found to be 24.9×10^6 psi $\pm$ 2%. The modulus was measured with the aid of strain gages mounted on both sides of each coupon. Because of the initial camber of the specimens cut from the cones, transverse stresses appeared when the specimens were straightened by the tension load. These secondary stresses (tension on the concave side and compression on the convex side) raised the measured value of E on the concave-side and lowered it on the convex-side. By averaging concave and convex values this effect was eliminated. The wall thickness of the shell was measured at 20 locations on the short shell and 64 locations on the long ones. The wall thickness was fairly uniform with variations always less then 7%.

Seven shells were tested. Four long ones of taper ratio $\psi = 0.750$ and three short ones of $\psi = 0.244$. The pressure was applied, as in Ref. 1, by slow evacuation at a rate of about 0.001 psi/sec. The geometries of the shells, the buckling pressure and correlation with theory are given in Table 1.

As is well known, the geometry of truncated conical shells is defined by the cone angle α, the radii of the small end R_1 and large end R_2, and the thickness h. Alternatively, one of the radii can be replaced by the slant length of the cone l. For comparison with cylindrical shells, the significant geometrical parameters are (ρ_{av}/h), where $\rho_{av} = (R_1 + R_2)/2 \cos\alpha$ is the average radius of curvature of the conical shell, (l/ρ_{av}) and a conicity parameter, the taper ratio $\psi = 1 - (R_1/R_2)$. The correlation between conical shells and equivalent cylindrical shells under hydrostatic pressure can be expressed by a correlation function g that is primarily a function of the taper ratio[2–4]

$$g(\psi) = (p_{cr}/\bar{p}) \tag{1}$$

where $\bar{p}$ is the critical pressure of an equivalent simply supported cylindrical shell of identical thickness for which $R = \rho_{av}$ and $L = l$. For moderate and long shells, $\bar{p}$ may be computed with an approximate formula[2,6] which for $\nu = 0.3$ becomes

$$(\bar{p}/E) = 0.918\ (h/\rho_{av})^{2.5}(\rho_{av}/l) \tag{2}$$

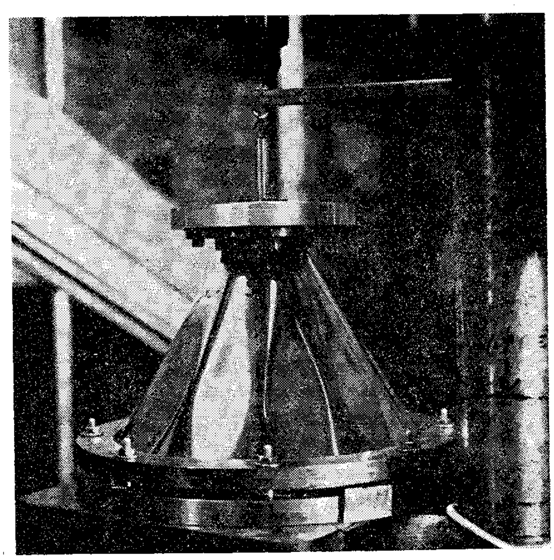

Fig. 1 Buckled long shell in test rig.

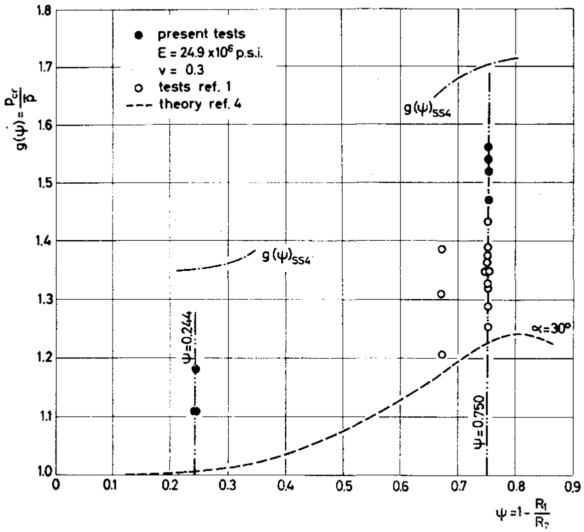

Fig. 2 Ratio of buckling pressures to that predicted for equivalent cylindrical shells on classical simple supports.

Since Eq. (2) is a simplification of the U.S. Experimental Model Basin formula given in Ref. 6, obtained by neglect of a negative term in the denominator that is small in comparison with (L/R), it is too conservative for short shells. Hence the complete formula should be employed in this case, which becomes for $\nu = 0.3$

$$(\bar{p}/E) = 0.918(h/\rho_{av})^{2.5}/[(l/\rho_{av}) - 0.636(h/\rho_{av})^{0.5}] \quad (3)$$

In order to be consistent $\bar{p}$ is computed with the complete formula, Eq. (3) for all shells in Table 1, though for the long shells the difference between the values obtained from Eq. (3) and Eq. (2) is less than 1%.

In the presentation of the results in Table 1 and Fig. 2, the emphasis is on the correlation function $g(\psi)$, whose behavior is being studied. In Table 1, $g(\psi)$ is therefore given both for the experimental results and for the calculated critical pressures. The theoretical values are for simple supports, but are obtained with a linear theory that takes the inplane boundary conditions into account.[7] For the "classical" SS3 B.C.'s the critical pressures are very close to those obtained in the earlier analyses[2,3] that do not comply rigorously with the inplane B.C.'s, and hence the correlation for this case is a direct continuation of that in Refs. 1–4. The present test conditions are between the "classical" SS3 and the complete axial restraint SS4 as in Ref. 1, and the test results again fall between the two cases, as can be seen in Table 1.

The correlation of $g(\psi)$ in Fig. 2 is, however, with equivalent cylindrical shells on classical simple supports and hence the experimental points are above the theoretical curve of Ref. 4. Segments of theoretical $g(\psi)_{ss4}$ curves have been outlined in Fig. 2. It should be noted that, since the stiffening due to axial restraint P_{ss4}/P_{ss3} varies considerably with the shell geometry parameter Z (see Fig. 6 of Ref. 7), $g(\psi)_{ss4}$ is represented here by a family of curves. On the other hand a single curve, for each range of cone angles, could be obtained by correlation with equivalent cylindrical shells having SS4 B.C.'s. The usefulness of such a redefined correlation function would, however, be doubtful.

It should also be mentioned here that one has to consider an (R_1/h) effect when one intends to apply the correlation curves to shells with small (R_1/h) as was pointed out in Ref. 4.

The test results are superimposed in Fig. 2 on the results of Ref. 1. The present test results are all higher than the corresponding ones of Ref. 1, on account of the larger axial restraint caused by additional tightening of the end rings for all the specimens.

In summary, as can be seen in Fig. 2, the present tests, that complement those of Ref. 1, but include also "control" specimens of small taper ratio, reconfirm and substantiate the "hump" in the correlation curve based on the linear theories of Seide and Singer for conical shells.

References

[1] Singer, J. and Bendavid, D., "Buckling of Electroformed Conical Shells under Hydrostatic Pressure," *AIAA Journal*, Vol. 6, No. 12, Dec. 1968, pp. 2332–2338; also SUDAAR Rept. 309, May 1967, Dept. of Aeronautics and Astronautics, Stanford Univ.

[2] Seide, P., "On the Buckling of Truncated Conical Shells under Uniform Hydrostatic Pressure," *Proceedings of the IUTAM Symposium on the Theory of Thin Elastic Shells*, North-Holland, Amsterdam, 1960, pp. 363–388.

[3] Singer, J., "Buckling of Conical Shells under Axisymmetrical External Pressure," *Journal of Mechanical Engineering Science*, Vol. 3, No. 4, Dec. 1961, pp. 330–339.

[4] Singer, J., "Correlation of the Critical Pressure of Conical Shells with That of Equivalent Cylindrical Shells," *AIAA Journal*, Vol. 1, No. 11, Nov. 1963, pp. 2675–2676.

[5] Singer, J. and Eckstein, A., "Recent Experimental Studies of Buckling of Conical Shells under Torsion and External Pressure," *Israel Society of Aeronautical Sciences, Conference On Aviation & Astronautics, 5th, Proceedings 1963*, Jerusalem Academic Press, Ltd., 1963, pp. 135–146.

[6] Batdorf, S. R., "A Simplified Method of Elastic Stability Analysis for Thin Cylindrical Shells," Rept. 874, 1947, NACA.

[7] Baruch, M., Harari, O., and Singer, J., "Effect of In-Plane Boundary Conditions on the Stability of Conical Shells under Hydrostatic Pressure," *Israel Journal of Technology*, Vol. 5, No. 1, Feb. 1967, pp. 12–25.